Progress In Electromagnetics Research C, Vol. 25, 145–157, 2012

A MAGNETIC FIELD TUNABLE YTTRIUM IRON GARNET MILLIMETER-WAVE DIELECTRIC PHASE SHIFTER: THEORY AND EXPERIMENT

M. A. Popov[1, 2], I. V. Zavislyak[1, 2], and G. Srinivasan[1, *]

[1]Physics Department, Oakland University, Rochester, MI 48309, USA

[2]Radiophysics Department, Taras Shevchenko National University of Kyiv, Volodymyrska 64, Kyiv 01601, Ukraine

Abstract—A magnetically tunable passive narrow-band split-mode mm-wave phase shifter based on dielectric resonance in yttrium iron garnet (YIG) is investigated. The novelty here is the demonstration of a phase shifter in the frequency region between two split dielectric resonances in YIG. It is shown that, under certain conditions, the differential phase shift from the split modes add up, resulting in a larger phase shift than for a single mode phase shifter. Two prototype phase shifters operating in the U- and W-bands at frequencies much higher than ferromagnetic resonance (FMR) in YIG have been designed and characterized. Phase shifts up to 30° with low losses and acceptable standing wave ratio are obtained for moderate bias magnetic fields. Equivalent transmission-line model taking into account coupling between the split resonances is presented and there is reasonable agreement between theory and experiment for both insertion loss and differential phase shift. Suggestions on further improvements of prototype filter characteristics have been outlined.

1. INTRODUCTION

Phase shifters are important elements in phased array radars and for applications in wireless communication, surveillance, sensing and tracking [1, 2]. Recently there has been considerable interest in signal processing at frequencies 70 GHz and higher [3]. Advantages associated with devices operating at such frequencies are enhanced band-width, improved resolution and directivity. A wide variety of materials

Received 14 October 2011, Accepted 8 November 2011, Scheduled 14 November 2011

* Corresponding author: Gopalan Srinivasan (srinivas@oakland.edu).

and devices based on semiconductors, ferroelectrics, and ferrites has been developed for high frequency applications [4–6]. In particular, phase shifters based on ferromagnetic resonance (FMR) or spin wave propagation in yttrium iron garnet (YIG) are attractive because of their planar geometry and magnetic tunability of their operating frequency over a wide range [2]. Yttrium iron garnet has long been used for device applications over 1–10 GHz because of low magnetic and dielectric losses. For frequencies above X-band, however, the need of large external magnetic fields makes the use of YIG less attractive for ferromagnetic resonance based devices.

This report constitutes a new proof-of-concept approach to magnetically tunable YIG phase shifter for use in the U- and W-band. It is based on dielectric resonances in a disk-shaped ferrite resonator. With proper choice of disk dimensions one can obtain the desirable operating frequency, well above FMR that facilitates a reduction in the insertion loss. Also there seems to be no physical or technical constraints for similar devices operating at hundreds of GHz. Such dielectric modes can be tuned with an external magnetic field due to ferromagnetic nature of the ferrites. Magnetic field tuning of the dielectric resonance frequency alters the mode characteristics, including the differential phase shift and insertion loss at a given frequency.

2. EXPERIMENTAL SET-UP

Two disks of YIG of dimensions diameter $D = 1.25\,\text{mm}$, thickness $S = 0.26\,\text{mm}$; and $D = 1.6\,\text{mm}$, $S = 0.46\,\text{mm}$ were used in the studies. For the larger disk (Sample A) lower-order dielectric resonance $E_{11\delta}$ [7] lies in the U-band (40–60 GHz), whereas for the smaller disk (Sample B) has the resonance in the W-band (75–110 GHz). YIG was chosen due to its excellent dielectric properties (dielectric losses tangent $\approx 2 \cdot 10^{-4}$ [8]) and low saturation magnetization (i.e., low tuning magnetic field). Room-temperature data on magnetization as a function of static magnetic field were obtained with a SQUID magnetometer and is shown in Fig. 1 for sample A. An identical M vs. H behavior was measured for Sample B.

Experimental set-up for studies on dielectric resonance in the YIG disks is schematically shown in Fig. 2(a). The disk was placed in the middle of the wide wall of an U- or W-band waveguide flange and fixed in place with polystyrene foam as shown in Fig. 2(b). The scattering matrix element measurements were made using Agilent Network Analyzers (model E8361A for U-band and N5242A with N5260A for W-band). Flanges with YIG disk could be considered as

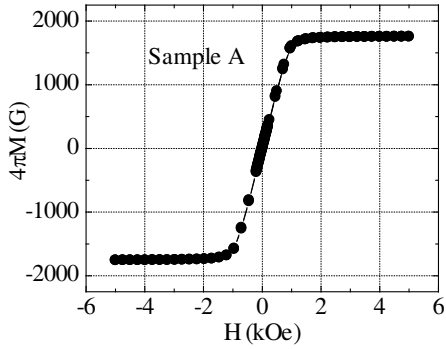

Figure 1. Magnetization versus static magnetic field H at room temperature for a single crystal YIG disk (Sample A). The static field was applied perpendicular to the sample plane.

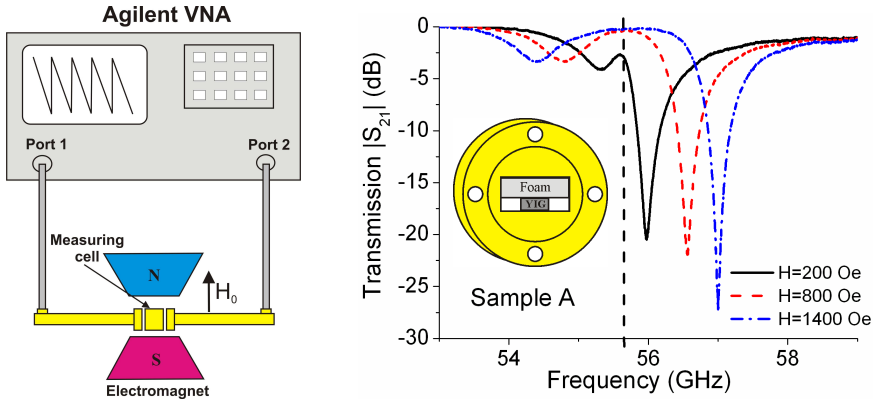

Figure 2. (a) Experimental set-up used for the observation of dielectric resonance in yttrium iron garnet (YIG). (b) Profiles of scattering matrix parameter S_{21} versus frequency f showing the dielectric resonance in a disk of YIG. Two modes, corresponding to clockwise and counter-clockwise polarization of microwave fields, are seen. With increasing bias field H, notice the up-shift in one mode and a down-shift the other mode of the split modes. The inset shows the YIG disk in a waveguide flange.

a prototype of the phase shifter and its characteristics were measured over the whole frequency band under bias magnetic fields. The applied bias field H was perpendicular to the disk surface.

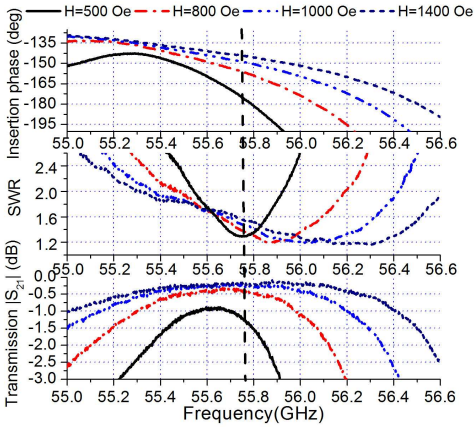

Figure 3. Phase angle, standing wave ratio (SWR) and insertion loss as a function of frequency for a series of bias fields H for the YIG disk (sample-A). The vertical dashed line is guide to the eye indicating a differential phase shift with increasing H.

Typical $|S_{21}|$ vs. frequency f profiles for a series of H for Sample-A are presented in Fig. 2. For all bias fields two modes seen. The modes correspond to clockwise and counter-clockwise polarization of the microwave fields [9–12]. Although the theory [12] predicts degenerate modes for $H = 0$, zero-field splitting is observed in Fig. 2 due to the presence of large domains [12]. With an increase in H, one notices an up-shift in the frequency of one mode and a down-shift in the other. Frequencies of these modes lie in the U-band, well above the FMR frequency of 1–5 GHz for the biasing fields for the profiles in Fig. 2.

Next we consider a narrow region of frequency between the split modes. Fig. 3 shows the profiles over 55–56.6 GHz in an expanded scale. Data on frequency dependence of parameters of importance for a phase shifter, i.e., phase, insertion losses, and standing wave ratio (SWR), over this frequency range are shown for a series of bias field H in Fig. 3. Note that H does not start from zero, but from $H = 500$ Oe, so that zero-field losses could be eliminated. The choice of operating frequency for H-tunable phase shifter is determined by combination of low insertion loss, large phase shift, and low SWR. From this consideration it is clear that for U-band the operating point is ideally around 55.8 GHz. At this frequency, H tuning gives a differential phase shift of 31°, SWR < 1.54, and insertion loss of 0.3–1.25 dB. Calculations show that out of this total insertion loss, 0.1–0.2 dB is attributed to impedance mismatch. Hence, better matching

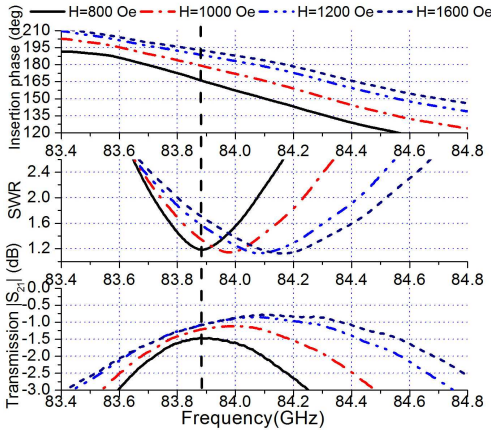

Figure 4. Data as in Fig. 3, for YIG disk (sample-B) in the W-band.

will improve losses, though not substantially. Nevertheless, current configuration still provides substantial figure-of-merit, $\sim$ 24.6°/dB. Characteristics of the W-band phase shifter, operating at 83.9 GHz frequency, are shown in Fig. 4 and are found to be quite similar the data in Fig. 3. Losses in Fig. 4 are higher, ranging from 1 to 1.5 dB and phase shift is 28°, thus giving somewhat lower figure-of-merit of 18.6°/dB. Thus with appropriate sample dimensions it is possible to design a H-tunable phase shifter based on dielectric resonance in YIG. Achievable frequency range can be from tens of GHz to sub-THz.

3. THEORETICAL MODEL AND CALCULATIONS

Theoretical models that consider electromagnetic modes in axially magnetized cylindrical ferrite resonators [9–12], predict that modes with nonzero azimuthal index, e.g., $E_{+11\delta}$ and $E_{-11\delta}$, excited by clockwise and counterclockwise microwave fields are degenerate for $H = 0$. However, this degeneracy is removed in a bias field and their frequencies become H dependent due to change in static permeability. In order to find the insertion loss and phase shift, we shall describe our two-resonance system by an equivalent transmission-line model shown in Fig. 5 [13–15]. Each resonance will correspond to a separate series resonant circuit with an equivalent inductance and capacitance that define the resonant frequency, and an equivalent resistance that determines insertion losses.

If one assumes a infinite conductivity for metal wall on which the YIG disk is placed, then split eigen-modes are orthogonal and,

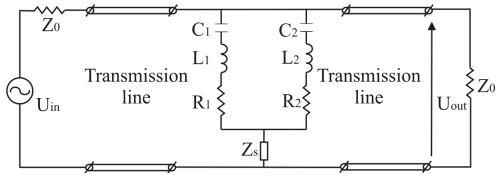

Figure 5. Equivalent transmission-line model for two-mode dielectric resonance in YIG disks.

therefore, are not coupled. However, in metals with finite conductivity coupling between the modes will occur [16]. To reflect this fact, an additional circuit element Z_s is added in Fig. 5. The surface impedance of waveguide wall $Z_s = R_s + iX_s = \sqrt{\frac{\omega\mu_r\mu_0}{2\sigma}}(1+i)$ (in SI units) [13], and the resistive and reactive components of the complex impedance are equal $R_s = X_s$. Thus, we will assume that $Z_s = R_s(1+i)$. Whereas R_1 and R_2 represent dielectric losses in the sample for a given mode, resistive component of surface impedance R_s stands for losses in waveguide wall and reactive part, X_s provides coupling between modes and frequency repulsion.

We will define transmission losses in dB as $20\lg(|U_{out}/U_{in}|)$, where U_{in} and U_{out} are input and output voltages at f (see Fig. 5). Similarly, the phase is $\arg(U_{out}/U_{in})$. Using the circuit in Fig. 5, we obtain the complex transmission coefficient [17] close to resonance frequencies as:

$$\frac{U_{out}}{U_{in}} = \frac{1}{1 + \frac{\frac{K_1}{1+\xi_1} + \frac{K_2}{1+\xi_2}}{1 + M(1+i)\left(\frac{K_1}{1+\xi_1} + \frac{K_2}{1+\xi_2}\right)}} \tag{1}$$

where $K_i = Z_0/R_i$, $M = R_s/Z_0$, and $\xi_i = (f - f_{ri})/\Delta f_i$ is the normalized detuning factor. Here $f_{ri} = 1/(2\pi\sqrt{L_iC_i})$ is the resonance frequency of each series circuit, $\Delta f_i = f_{ri}/(2Q_i)$ is the resonance linewidth, and $Q_i = 2\pi f_{ri}L_i/R_i$ is the quality factor.

The theoretical estimates of loss characteristics were carried out in the following manner: first, Eq. (1) was fitted to the experimental transmission losses data (Fig. 2) until a minimum in root-mean-square error was achieved. After that, derived parameters were slightly adjusted in order to obtain the best possible match in the region of interest, between two resonance modes for a specific H. Attention was paid to three specific points: magnitude of losses at both resonance frequencies and position of minimum absorption between resonances.

Fitted loss vs f profiles are shown in Fig. 6 and the following parameters were used in Eq. (1) for the fitting: $M = 0.06$–0.08,

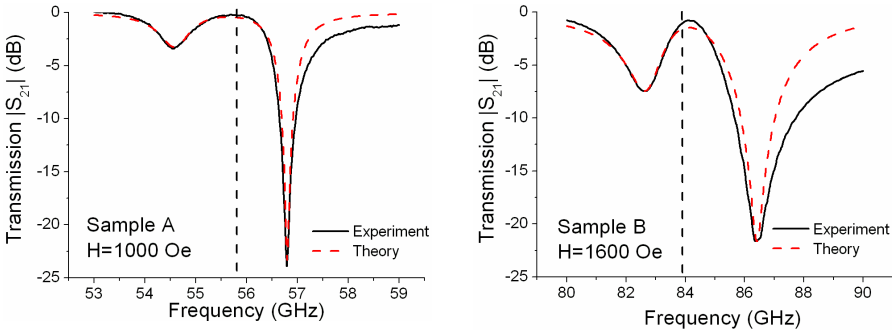

Figure 6. Measured loss vs. frequency (solid line) and theoretical fit calculated using Eq. (1) (dashed line) for Sample-A at $H = 1000$ Oe and for Sample-B at $H = 1600$ Oe.

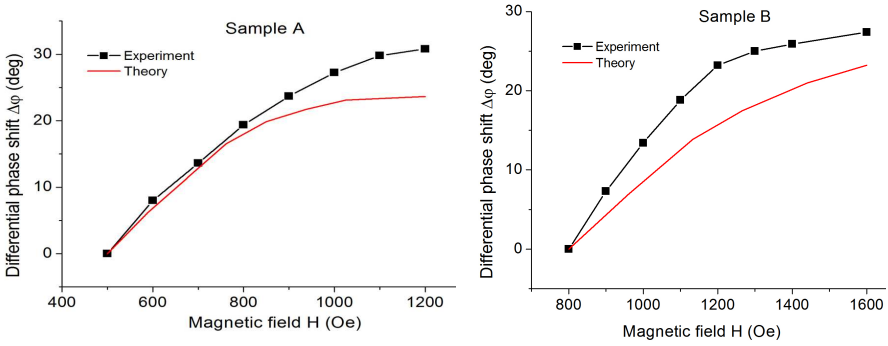

Figure 7. Comparison between measured differential phase shift and theoretical estimate for sample-A ($f = 55.8$ GHz) and sample-B ($f = 83.9$ GHz).

$K_1 = 0.5$–1.4, $\Delta f_1 = 0.35$–0.55 GHz, $K_2 = 150$–210, $\Delta f_2 = 0.01$–0.02 GHz.

It is noteworthy that the coupling parameter $M \sim 0.1$ which indicates a rather weak coupling. Also $K_2 \gg K_1$ and is due to much larger absorption for the higher frequency mode. Fitted resonance linewidth for high-frequency resonance was found to be 15 times smaller than for the low-frequency one and implies additional losses. As primary difference between resonances is in the eigen-mode polarization [18], the high losses are related to polarization-sensitive excitation of surface waves in the short [19].

The parameters determined from fits to $|S_{21}|$ vs. f curves were

substituted in Eq. (1) and the phase was calculated. Differential phase shifts, calculated by subtracting phase spectra at different values of magnetic bias field at some reference frequency, $\Delta\varphi(H) = \arg S_{21}(H) - \arg S_{21}(H_0)$ for Sample-A and Sample-B are compared with theoretical calculations in Fig. 7. One observes good agreement between data and estimates at low fields. That is not unexpected in view of the discrepancy between theoretical and measured transmission loss curves in Fig. 6.

4. DISCUSSION

Our theoretical model is used next to analyze the advantages of the two-resonance phase shifter. For the simplicity, we shall assume that resonances are not coupled ($M = 0$) and well separated ($\xi_1 \approx 1, \xi_2 \gg 1$ or vice versa). In this case the phase can be expressed in the form $\varphi_j = \text{arctg}(\frac{K_j \xi_j}{1+K_j+\xi_j^2})$, $j = 1, 2$ [15]. Corresponding plots are shown in Fig. 8. With the application of H, lower-resonance is down-shifted

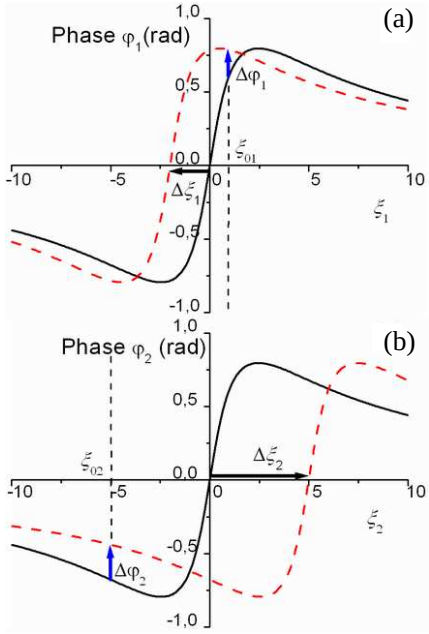

Figure 8. Phase angle for lower-frequency (a) and high-frequency (b) resonances with the application of a bias field H that results in down-shift in (a) and up-shift in (b).

and higher frequency resonance is up-shifted and the corresponding phase vs. f characteristics estimated with the substitutions $\xi_j \rightarrow \xi_j + (f_{rj}^{(1)} - f_{rj}^{(2)})/\Delta f_j = \xi_j + \Delta\xi_j$ are shown in Fig. 8.

Then, the total differential phase shift is $\Delta\varphi = \Delta\varphi_1 + \Delta\varphi_2$, where

$$\begin{aligned}\Delta\varphi_j &= \varphi_j^{(2)} - \varphi_j^{(1)} \\ &= \text{arctg}\left(\frac{K_j(\xi_j + \Delta\xi_j)}{1 + K_j + (\xi_j + \Delta\xi_j)^2}\right) - arctg\left(\frac{K_j\xi_j}{1 + K_j + \xi_j^2}\right) \\ &= \text{arctg}\left(\frac{K_j\Delta\xi_j(1 + K_j - \xi_j^2 - \xi_j\Delta\xi_j)}{(1 + K_j + (\xi_j + \Delta\xi_j)^2) \cdot \left(1 + K_j + \xi_j^2\right) + K_j^2\xi_j(\xi_j + \Delta\xi_j)}\right).\end{aligned}$$

From the above equation one can easily infer that for decreasing resonance frequency $\Delta\varphi_j > 0$, when operating point $-\sqrt{\Delta\xi_j^2/4 + K_j + 1} - \Delta\xi_j/2 < \xi_{oj} < \sqrt{\Delta\xi_j^2/4 + K_j + 1} - \Delta\xi_j/2$ and $\Delta\varphi_j < 0$ otherwise.

In our experiments, the shift in resonance frequencies $f_{rj}^{(1)} - f_{rj}^{(2)}$ for all cases (see Fig. 2) is less then 0.8 GHz, whereas resonance linewidths are quite different. For high-Q higher resonance frequency increase and detuning factor $\xi_{o2} \ll -1$, due to $\Delta f_2 \ll |f_o - f_{r2}|$, therefore phase shift $\Delta\varphi_2$ is always positive. On the other hand, for lower resonance fitted ΔF_1 was found to be 0.3–0.5 GHz, thus ξ_{o1} is small and positive. As we can see from Fig. 8, and above-mentioned expressions, there is a range of small positive detuning for which differential phase shift $\Delta\varphi_1$ from first resonance is positive. At given frequency f_0 the largest phase shift $\Delta\varphi_1$ is for relatively small change in resonant frequency; for larger $\Delta\xi_1$ it will decrease and finally become negative. Thus, for given ξ_{o1} there is a frequency shift range $0 < \Delta\xi_1 < (\Delta\xi_1)_{\max} = (K_1 + 1 - \xi_{o1}^2)/\xi_{o1}$ for which presence of lower-frequency resonance will be a positive factor for net phase shift $\Delta\varphi$.

In summary, if the operating point f_0 is chosen such that it corresponds to $\xi_{o2} \ll -1$ and simultaneously $\xi_{o1} \approx 1 - 2$, differential phase shifts from both resonances $\Delta\varphi_1$, $\Delta\varphi_2$ would be positive and add up for some range of magnetic field. Take note that if both split modes have comparable linewidth Δf, this situation would be impossible since $\xi_{o1} \approx \xi_{o2}$. But in our case noted above specific feature of split resonances in disk on waveguide wall with drastically different Q factors plays decisive role, and operation between resonances will yield larger tunable phase shift than in the cases of single resonance explored in earlier reports [20, 21].

The phase shifter discussed here has a figure-of-merit (FOM),

approximately 25°/dB at U-band and 19°/dB at W-band. It is comparable with FOM for semiconductor-device based phase shifters [22–24], however is inferior to MEMS phase shifters [25]. Therefore, the only way to increase FOM is by decreasing losses by polishing the sample. Desired phase shifts can be achieved by combining multiple identical disk resonators in the waveguide section. By placing samples at $3\lambda/4$ distance between centers, a 180° section can be achieved with a 24 mm long at U-band waveguide and a 17 mm long W-band waveguide.

Magnetic field at which phase shift reaches saturation is 1400 Oe for Sample-A and $\approx$ 1600 Oe for Sample-B. That is, in essence, the saturation field $H_{sat} = 4\pi M_s \cdot N_{zz}$, N_{zz} the demagnetizing factor [26], when domain structure is suppressed and sample is under saturation. At this point frequency tuning due to changes in net magnetization is zero, and all subsequent variation of resonance frequency (and phase, respectively) will be very small. That implies that required bias field range is, basically, $H < H_{sat}$, and by no means bound to FMR condition. Thus, to decrease the external field for phase tuning one needs to use Gd-substituted YIG with lower $4\pi M_s$ and/or a sample with larger thickness to radius ratio to decrease longitudinal demagnetizing factor N_{zz}.

In YIG samples zero-field splitting of counter rotating mode frequencies is present, contrary to observations for dielectric resonance in barium hexaferrites (BaM) disks [7]. It could be a consequence of differences in the domain structures [12, 27, 28]; domains in BaM are much smaller and after spatial averaging its zero-field high-frequency properties more resemble a pure dielectric. Such splitting may be considered as an advantage, since it creates low-loss operating region between resonances without applied field and, thus, decreases minimum required magnetic field. It is quite possible that for some materials and/or sample shapes initial splitting due to specific domain structure will permit phase shifter operation starting from zero bias. Also, it is worth mentioning that this ferrite phase shifter is based on dielectric resonances, and not on FMR. High power nonlinear losses are inherent to spin-wave devices [29, 30]. Such losses are absent in our case and the phase shifter can handle very high RF power.

5. CONCLUSION

A prototype magnetic field tunable phase shifter based on dielectric resonance in the U-band and W-band has been investigated. Phase shifters utilize yttrium-iron garnet, a material widely used for devices at much lower frequencies. However, the devices discussed here are not

based on FMR, but on magneto-dielectric resonances corresponding to clockwise and counter-clockwise polarizations. With the application of H the modes diverge, with one showing up-shift and the other down-shift. Magnetic tuning of resonance frequency causes changes in phase at a given frequency. Selection of operating frequency roughly between split resonances ensures low losses and summation of contributions from both resonances to differential phase shift.

The phase shifters with operating frequencies 55.8 and 83.9 GHz have phase shifts of approximately 30°, insertion loss of 0.2–1.2 dB at U-band and 1–1.5 dB at W-band, and SWR less than 1.6. Tuning bias fields in both cases are rather moderate, about 1600 Oe. An equivalent transmission-line model was proposed, taking into account coupling between the modes via surface impedance of waveguide walls. This model provides satisfactory agreement with data.

ACKNOWLEDGMENT

The work at Oakland University was supported by grants from the Army Research Office and the Office of Naval Research.

REFERENCES

1. Romanofsky, R. R., "Array phase shifters: Theory and technology," NASA Glenn Research Center, Cleveland, OH, Technical Memorandum NASA/TM—2007-214906, 2007.
2. Adam, J. D., L. E. Davis, G. F. Dionne, E. F. Schloemann, and S. N. Stitzer, "Ferrite devices and materials," *IEEE Trans. MTT*, Vol. 50, No. 3, 721–737, Mar. 2002.
3. Vizard, D. R., "Millimeter-wave applications: From satellite communications to security systems," *Microwave Journal*, Vol. 49, 22–36, 2006.
4. Cole, M. W., W. D. Nothwang, S. Hirsch, E. Ngo, C. Hubbard, and R. G. Greyer, "High performance thin films for microwave phase shifter applications: Device requirements, material design, and process science considerations," *Ceramic Transactions*, Vol. 174, 287–296, 2006.
5. Kuanr, B., Z. Celinski, and R. E. Camley, "Tunable high-frequency band-stop magnetic filters," *Appl. Phys. Lett.,* Vol. 83, 3969–3971, 2003.
6. He, P., P. V. Parimi, Y. He, V.G. Harris, and C. Vittoria, "Tunable negative refractive index metamaterial phase shifter," *Electronics Letters*, Vol. 43, No. 25, 1440–1441, Dec. 2007.

7. Popov, M., I. Zavislyak, A. Ustinov, and G. Srinivasan, "Sub-Terahertz magnetic and dielectric excitations in hexagonal ferrites," *IEEE Trans. on Mag.*, Vol. 47, No. 2, 289–294, Feb. 2011.
8. Krupka, J., S. A Gabelich, K. Derzakowski, and B. M. Pierce, "Comparison of split post dielectric resonator and ferrite disc resonator techniques for microwave permittivity measurements of polycrystalline yttrium iron garnet," *Meas. Sci. Technol.*, Vol. 10. No. 11, 1004–1008, Nov. 1999.
9. Bosma, H., "On stripline Y-circulation at UHF," *IEEE Trans. on MTT*, Vol. 12, No. 1, 61–72, Jan. 1964.
10. Gibson, A. A. P., B. M. Dillon, and S. I. Sheikh, "Applied field/frequency response of planar gyromagnetic disks," *Int. J. Electronics,* Vol. 76, No. 6, 1073–1081, Jun. 1994.
11. Schieblich, C., "Mode charts for magnetized ferrite cylinders," *IEEE Trans. on MTT*, Vol. 37, No. 10, 1555–1561, Oct. 1989.
12. Popov, M. A., I. V. Zavislyak, and G. Srinivasan, "Sub-THz dielectric resonance in single crystal yttrium iron garnet and magnetic field tuning of the modes," *J. Appl. Phys.*, Vol. 110, No. 2, 024112-1–024112-7, Jul. 2011.
13. Chen, L. F., C. K. Ong, C. P. Neo, V. V. Varadan, and V. K. Varadan, *Microwave Electronics. Measurement and Material Characterization*, Ch. 1.2, Ch. 2.2, John Wiley & Sons, Ltd., Chichester, England, 2004.
14. Pozar, D. M., *Microwave Engineering*, 2nd edition, Ch. 2.1, John Wiley & Sons Inc., New York, 1998.
15. Ilchenko, M. E. and E. V. Kudinov, *Ferritovye i Dielectricheckye Resonatory SVCh*, Ch. 3.4, Izdatelstvo Kievskogo Universiteta, Kiev, 1973 (in Russian).
16. Ilyinsky, A. S., G. Y. Slepyan, and A. Y. Slepyan, *Propagation, Scattering and Dissipation of Electromagnetic Waves*, 86–90, Peter Peregrinus Ltd., Wiltshire, UK, 1993.
17. Gurevich, I. V., *Osnovi Raschetov Radiotechnicheskih Cepey*, Ch. 3, Svyaz, Moscow, 1975 (in Russian).
18. How, H. and C. Vittoria, "Microwave phase shifter utilizing nonreciprocal wave propagation," *IEEE Trans. on MTT*, Vol. 52, No. 8, 1813–1819, Aug. 2004.
19. Chiu, K. W. and J. J. Quinn, "Magnetoplasma surface waves in metals," *Phys. Rev. B*, Vol. 5, No. 12, 4707–4709, Jun. 1972.
20. Popov, M. A., I. V. Zavislyak, and G. Srinivasan, "Magnetic field tunable 75–110 GHz dielectric phase shifter," *Electronics Letters*, Vol. 46, No. 8, 569–570, Apr. 2010.

21. Tatarenko, A. S., G. Srinivasan, and M. I. Bichurin, "Magnetoelectric microwave phase shifter," *Appl. Phys. Lett.*, Vol. 88, No. 18, 183507-1–3, May 2006.
22. Nam, S., A. W. Payne, and I. D. Robertson, "RF and microwave phase shifter using complementary bias techniques," *Electronic Letters*, Vol. 37, No. 18, 1124–1125, Aug. 2001.
23. Tsai, M.-D. and A. Natarajan, "60 GHz passive and active RF-path phase shifters in silicon," *IEEE Radio Frequency Integrated Circuits Symposium (RFIC)*, 223–226, 2009.
24. Yu, Y., P. G. M. Baltus, and A. H. M. van Roermund, "A 60 GHz passive phase shifter," *Analog Circuits and Signal Processing*, Vol. 1, 47–58, 2011.
25. Afrang, S. and B. Yeop Majlis, "Small size Ka-band distributed MEMS phase shifters using inductors," *Progress In Electromagnetics Research B*, Vol. 1, 95–113, 2008.
26. Joseph, R. I. and E. Schlomann, "Demagnetizing field in nonellipsoidal bodies," *J. Appl. Phys.*, Vol. 36, No. 5, 1579–1593, May 1965.
27. Schlomann, E., "Microwave behavior of partially magnetized ferrites," *J. Appl. Phys.*, Vol. 41, No. 1, 204–214, Jan. 1970.
28. Schlomann, E., "Behavior of ferrites in the microwave frequency range," *J. Phys.*, Vol. 32, No. 2–3, 443–451, Feb.–Mar. 1971.
29. Zahwe, O., B. Abdel Samad, B. Sauviac, J. P. Chatelon, M. F. Blanc Mignon, J. J. Rousseau, M. L. Berre, and D. Givord, "YIG thin film used to miniaturize a coplanar junction circulator," *Journal of Electromagnetic Waves and Applications*, Vol. 24, No. 1, 25–32, 2010.
30. Zahwe, O., B. Sauviac, and J. J. Rousseau, "Fabrication nad measurement of a coplanar circulator with 65 μm YIG thin film, *Progress In Electromagnetics Research Letters*, Vol. 8, 35–41, 2009.